Chen, W., Liu, J., Li, F., Cao, X., Li, J., Zhu, X., and Chen, Q. 2017. "Ventilation similarity of an aircraft cabin mockup with a real MD-82 commercial airliner," *Building and Environment*, 111: 80-90.

Ventilation similarity of an aircraft cabin mockup with a real MD-82 commercial airliner

Wenhua Chen[a], Junjie Liu[a,*], Fei Li[a], Xiaodong Cao[a], Jiayu Li[a], Xueliang Zhu[a] and Qingyan Chen[a, b]

[a]Tianjin Key Laboratory of Indoor Air Environmental Quality Control, School of Environmental Science and Engineering, Tianjin University, Tianjin, China
[b] School of Mechanical Engineering, Purdue University, West Lafayette, Indiana, USA

[*]Corresponding author. Room 228, Building 14, Tianjin University, Tianjin, 300072, China.
[*]*Corresponding email: jjliu@tju.edu.cn*

Abstract: Most experimental studies on the aircraft cabin environment were conducted in aircraft cabin mockups. The ventilation differences between the cabin mockups and real cabins is always contentious and has not been identified. Measurements were made to determine the ventilation differences in two cabin facilities with the same single aisle layouts and similar diffuser structures, an MD-82 commercial airliner and a cabin mockup based on the Boeing 737. The ventilation performance of the two cabins, including the ventilation rate, mass balance and air velocity, were compared based on the data collected by ultrasonic anemometers (UAs). The result showed that the two cabins met the requirement of the ASHRAE standard, and the cabin mockup was sufficient to reflect the longitudinal flow in real cabins. The air velocity fields measured by UAs and 2D particle image velocimetry (PIV) in the cabin mockup were compared. Suggesting that the difference introduced by different measurement methods could be ignored, and the simplified diffuser geometry in the cabin mockup had no significant effect on the airflow. The requirement to maintain a certain type of airflow pattern in the cabins was analyzed by calculating the modified Reynolds number (Re) and Archimedes number (Ar), and it was found that the cabin mockup had similar air distribution features as the MD-82. These similar phenomena and similitude criteria verified that this cabin mockup is accurate enough to represent a real cabin environment and could be better used in the study of ventilation.

Key words: Aircraft cabin; Airflow pattern; PIV; Similitude criteria; UA; Ventilation similarity.

Nomenclature

g	acceleration of gravity, m/s^2
T_f	temperature of the heated floor, K
T_i	temperature of the inlet air, K
β	thermal expansion coefficient of air, $\beta = 2/(T_f + T_i)$, 1/K
ΔT_0	temperature difference between the inlet and floor, K
L	width of the cabin, m

H	height of the cabin, m
u_0	air velocity of the inlet, m/s
w	width of the diffuser, m
h	height of the diffuser, m
Q	ventilation rate, m^3/h
C_d	diffuser discharge coefficient
L_p	penetration distance of the wall jet, m

1. Introduction

The number of international tourists was over 1 billion (1.035 billion) in 2012 [1]. Aircrafts are surrounded by low temperature (-50 °C) and pressure (0.3 atm.) atmosphere when cruising at an altitude of 8400-12500 m. The airliner cabin environment needs to be considered many environmental factors and well designed to ensure travelers' safety, health, and comfort. Zhu et al. [2] conducted a field study on 10 trunk airlines in China. They reported some passengers had complained about their thermal conditions, especially in feeling warm, and most of the discomfort was caused by the low air velocity. Li et al. [3, 4] reported that a contaminant released in the middle row may be transmitted to the front and back rows of a real MD-82 commercial airliner because of the longitudinal flow. Hence, it is requisite to investigate the air distributions in airliner cabins.

Researchers have paid great attention to experimental research on the air distribution in aircraft cabins, including mockups and real aircraft cabins. Liu et al. [5] provided a procedure to obtain the precise boundary conditions and high quality flow fields in the first class cabin of an functional MD-82 commercial airliner. Shen et al. [6] and Li et al. [7] also obtained accurate cabin airflow turbulent dynamic characteristics and investigated the thermal environment and contaminant transport in the economy class of a commercial airliner. However, most of the measurements were conducted in mockup aircraft cabins [8-15] because of economic considerations. The mockup geometry and air supply system always employed some simplifications because of the level of processing techniques, and the simplification, compared with real cabins, may make the experimental result less valuable. Some studies [16] adopted mockups that were generic replicas of real cabins and failed to provide data from the occupied area. Some studies used cabin mockups without seats or heated manikins [10, 17, 18]. All these simplifications led to a discrepancy between the mockup and real aircraft cabin. Therefore, whether a mockup can be accurate enough to represent the real cabin environment is always contentious. It is important to compare the cabin mockup and a real cabin to determine the airflow differences caused by the simplifications.

For the comparison, accurate and high quality flow field data needed to be acquired, and the appropriate measuring instruments were selected. Liu et al. [19] reviewed previous experimental measuring techniques to obtain the cabin jet flow information. In general, the information is available using point-wise and global-wise measuring techniques. Point-wise measuring techniques is based on Newton's law for cooling, optic principles and acoustic principles. Examples of instruments include hot-wire anemometer (HWA) [20], hot-sphere anemometer (HSA) [21] and ultrasonic anemometer (UA) [5, 6, 14, 22]. Accurate

three-dimensional airflow information can be provided with UA, and it is easy to place and move in a cabin. This paper chooses UAs to measure the flow field of complete sections in a cabin mockup and a real cabin under cruise conditions. Compared with point-wise measuring techniques, global-wise measuring techniques can obtain the full-field velocity field and relevant statistical information without disturbing the airflows using techniques such as particle image velocimetry (PIV) [8, 9, 11, 23-25] and particle tracking velocimetry (PTV) [26, 27]. Because of the large measuring area, higher resolution and time savings, we also applied a high-power 2D-PIV system devoted to studying complex jet flows in a cabin mockup.

In practice, some boundary conditions of the cabin mockup and real cabin are not strictly the same, so the airflow fields could not be compared directly. Dimensional analysis is used to consider all relative parameters on the airflow quantitatively. The Reynolds number (Re) of the inlets had to be used as the similitude criterion [28-33] for airflow in an isothermal mixing ventilated room. The Archimedes number (Ar) was demonstrated to be the dominant variable for the pattern in a non-isothermal mixing ventilated enclosure [34, 35], taking into account the influence of the height and width of the room. Tripathi et al. [36] studied the air drafting pattern in a room by varying the Reynolds number and Archimedes number. As we know, the mixing ventilation (upper supply and bottom return) is the conventional and mainstream ventilation systems in real cabins [10], regardless of what type it is. So we just focused on the mixing ventilation in this paper, by considering the influence of the geometry and air supply characteristics of the cabin, the Reynolds number and Archimedes number were modified and used to describe the airflow patterns.

Thus, the major objective of this work was to synthetically quantify the two criteria in the cabins through the experiment and apply the modified Re and Ar to evaluate the airflow in the cabins. This study also provided a method procedure and similitude criteria to compare the airflow in cabin mockups and real cabins. For this purpose, the comparability of the airflow in the two cabins needed to be guaranteed. First, the characteristics of the ventilation performance, including the ventilation rate, mass balance and air velocity, were analyzed and compared. Then, the difference introduced by different measurements was calculated to assure the reliability of the experimental data. Moreover, the original diffuser in the cabin mockup was modified like the diffuser of the MD-82. The small effect of the simplified diffusers on the airflow was verified by comparing the flow field obtained in the upper area of parts of the cross section.

2. Research method

2.1 Cabin ventilation facilities

This research was carried out in two different cabin facilities with the same single aisle layouts and similar diffuser structures, an aircraft cabin mockup based on the Boeing 737 and an MD-82 cabin. As shown in Fig. 1, the cabin mockup was placed in a thermostatic chamber, and the cabin air was supplied by an air handling unit (AHU). The dimension at the deck level was 5.5 m (length) × 3.53 m (width), with a ceiling height of up to 2.15 m from the deck, and the deck was equipped with 42 manikins to simulate in-flight conditions. The MD-82 cabin supplied air through a ground air-conditioning cart (GAC). The dimension at

the deck level was 5.6 m (length) × 3.15 m (width), with a ceiling height of up to 2.05 m from the deck, and the deck was occupied by 35 manikins to simulate in-flight conditions.

The geometries and parameters of the air supply boundary conditions are shown in Fig. 2. In the cabin mockup, the ventilation system had a ceiling-supplied air duct and two side-supplied air ducts mounted at the luggage compartment level. The air was exhausted from the outlets on the side wall at the deck level. The seven pieces of air diffusers contained a total of 766 linear slots mounted on each side-supplied air duct. A honeycomb screen [11] was added inside each side-supplied air duct to achieve a uniform fluid boundary condition and reduce the inlet turbulence intensity. In the MD-82, the seven pieces of air diffusers contained a total of 980 linear slots mounted on each side-supplied air duct.

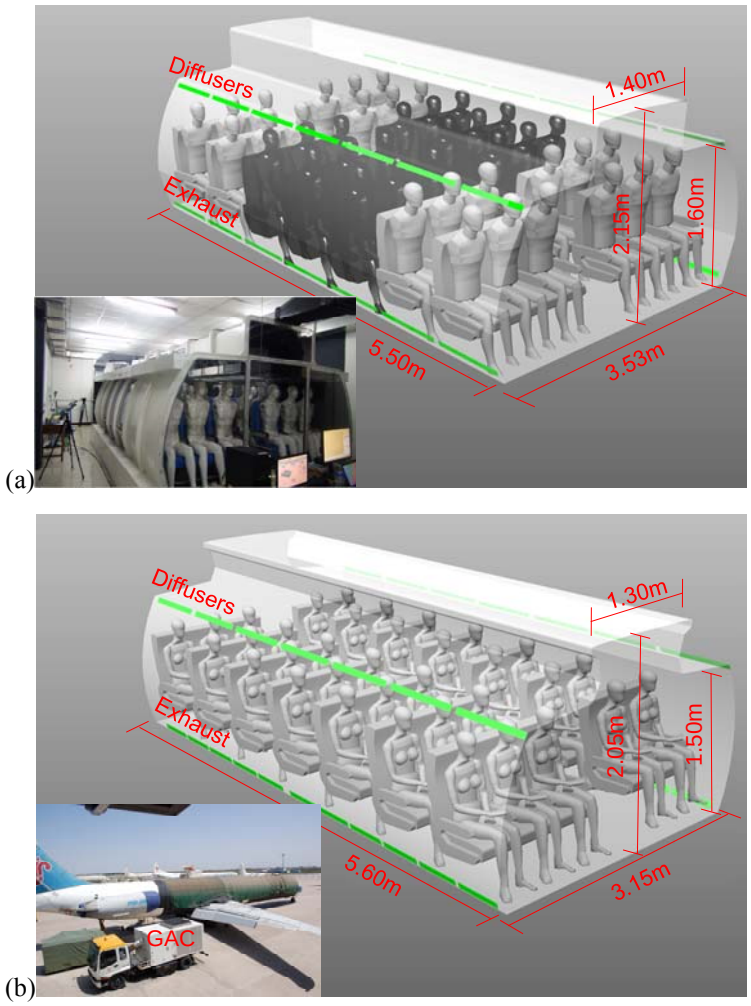

Fig. 1. Schematic of the experimental platforms: (a) cabin mockup and (b) MD-82.

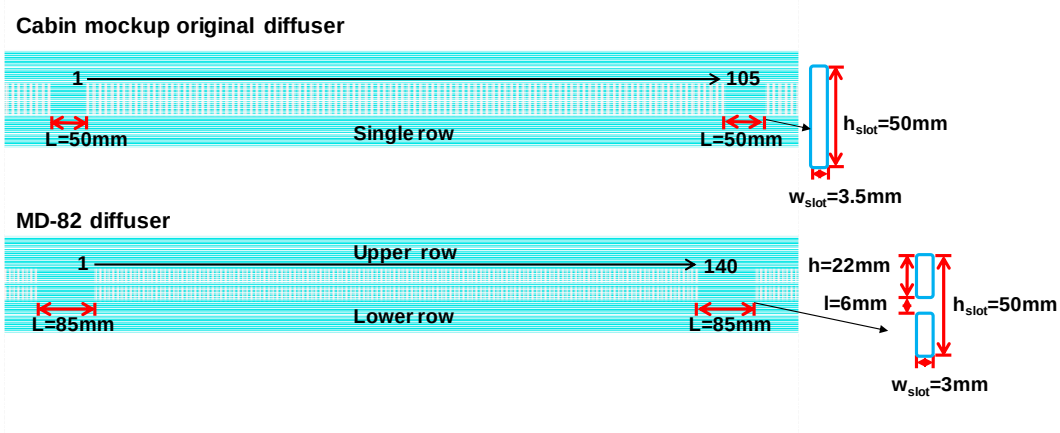

Fig. 2. Linear slot diffusers of the cabin mockup and MD-82.

In an aircraft cabin, a minimum air supply of 7.1 L/(per•s) is required, and a minimum air supply of 9.4 L/(per•s) is recommended by ASHRAE [37]. In the cabin mockup, the supplied air temperature was set at 19 ± 0.2 °C. And the supply air volume was controlled to be 1420 ± 60 m^3/h, which was equal to 9.4 L/(per•s). The cabin mockup was placed in a thermostatic chamber, and the ambient air temperature was set 19±1 °C. In the MD-82, the supplied air temperature was controlled at 18.3 ± 0.2 °C. The supply air volume corresponded to 7.1 L/(per•s), and this value was less than the cabin mockup. The most possible reason for this discrepancy was that the MD-82 is a decommissioned airliner, and the air supply parameters should be lower than the current standard. However, they both met the ASHRAE standard [37]. The outdoor air temperature changed from 19 to 35 °C. The indoor temperature boundary was controlled, and the exhaust airflow temperature fluctuated in the range of 22.8-23.8 °C during the experimental period. Therefore, the insulation materials successfully maintained a constant cabin air temperature. Our measurements showed that the manikin power input was within the range of the design value, and it was approximately 75 ± 5 W in the two cabins, in accordance with real human heat production.

2.2 Ventilation experimental set-up

In the cabin mockup, a high-power 2D particle image velocimetry testing system was used for the jet flow field measurement, consisting of an Neodymium-doped Yttrium Aluminium Garnet (Nd: YAG) laser and an 11 M-pixel charge coupled device (CCD) camera. Restricted by the film size, the cross-section flow field was separated into five reasonable zones, almost covered the full cross-section. An overlapping region 100 mm long was set between adjacent zones to reduce the joint errors. The measured cross-section was located at the middle points of Rows 3 to 5, and it was approximately 10 mm away from the manikin face.

Liu et al. [5] noted that the impact of the front and back ending walls can be neglected for the middle row. To remove errors due to background noise in the calculation, the manikins in Row 3 and Row 5 were painted black. The stage smoke oil was evaporated into 1.5 μm diameter smog by a PT-1000 evaporator-condensing smog generator.

One-hundred-and-eighty films were set as the statistical sample and calculated with a high precision sub-pixel difference algorithm to work out the flow field results.

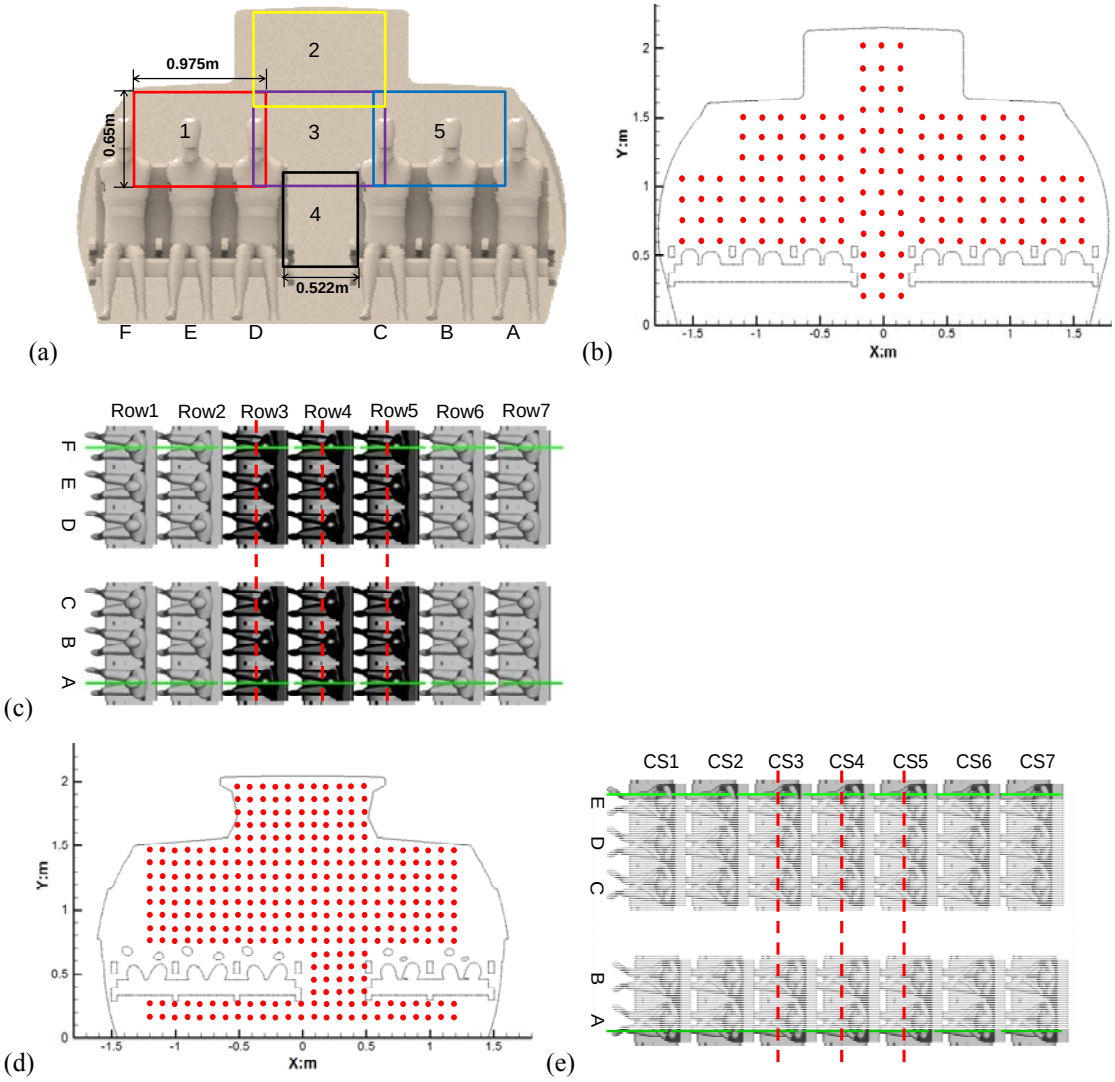

Fig. 3. (a) Composition of the PIV measurement regions (Cao et al., 2014), (b) the resolution of the measured points by the UAs in the cabin mockup, (c) locations of the measured planes in the cabin mockup, (d) the resolution of the measured points by the UAs in the MD-82, and (e) locations of the measured planes in the MD-82.

As shown in Fig. 3(c), the flow fields were measured in the three cross-sections (Row 3-Row 5) to almost obtain the complete airflow information above the chests, including the detailed characteristics of the inlet jet from the diffusers, because of the high measurement resolution. UAs [5, 6] had also been used for the flow field measurement with the same method in a cabin and acquiring data in the occupied zone, which PIV cannot obtain because of its flexibility. Fig. 3(b) shows the grid resolution used for the measurements, and the sampling grid resolution was 0.15 m × 0.15 m for the measured planes. In the MD-82, the flow fields were also measured by UAs in three cross sections, as shown in Fig. 3(e). Fig. 3(d)

shows the grid resolution used for the measurements, and the sampling grid resolution was 0.1 m × 0.1 m for the measured planes. There were 147 points for the cabin mockup and 227 points for the MD-82.

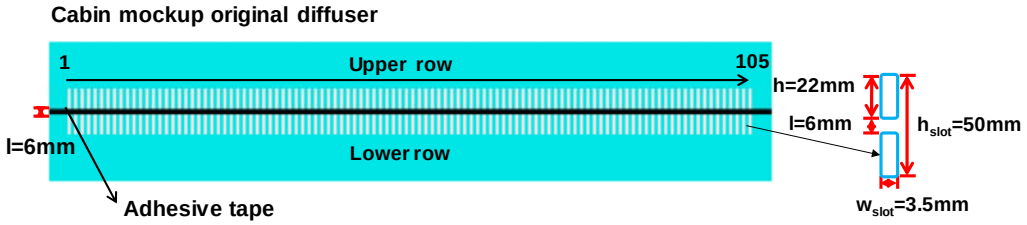

Fig. 4. Schematic model of the modified diffuser in the cabin mockup

As shown in Fig. 2, the linear slot diffusers were arranged in two rows in the MD-82. However, there was a single row in the cabin mockup. Therefore, to find the difference between the two linear slot diffusers in the two cabins, adhesive tape was used to divide the slot of the original diffuser into two parts, and the size of the adhesive tape was 6 mm. Figure 4 shows the schematic model of the modified diffuser in the cabin mockup. Under an isothermal condition and with the same air supply volume, the velocity fields of the two diffusers were measured by PIV in part 5 (Row 4).

2.3 Theoretical considerations

The Archimedes number is a dimensionless characteristic parameter describing the interaction between forced convection and natural convection on the air jet. Under a non-isothermal condition, based on the theoretical analysis of Wang et al. [34], Yu [35] modified the Archimedes number to predict the air drafting pattern in a ceiling slot-ventilated room:

$$Ar = \frac{g\beta\Delta T_0 h}{u_0^2} \tag{1}$$

The w/h value of the inlet exceeded 20, and the flow was two-dimensional. Therefore, the height of the inlet was chosen as the characteristic length. Fig. 1 shows the height and length of the different cabin plane sizes are not the same, so only considering the influence of the airflow by the inlet was not enough. In the cabin, under the ideal supply air condition, the airflow pattern can be divided by the middle line of the aisle. On the measured section, the airflow was hindered by thighs and chairs, and on the other hand, the air velocity was near zero at the area up the wall of the baggage holder [9]. Thus, the affected area of the single side wall jet was defined as shown in Fig. 5(a), and the characteristic dimension of the Archimedes number was defined as $\sqrt{HL}$. T_f corresponded to the surface temperature of the manikins, reflecting the effect of the thermal buoyancy by the passengers. Moreover, the measurement interface can be affected by multiple slots. u_0 is defined as being equal to the mean velocity of the multiple slots diffusers. Therefore, in the cabin, $Ar_{section}$ under a two-dimensional flow can be defined as:

$$Ar_{section} = \frac{g\beta\Delta T_0 \sqrt{F}}{u_0^2} \tag{2}$$

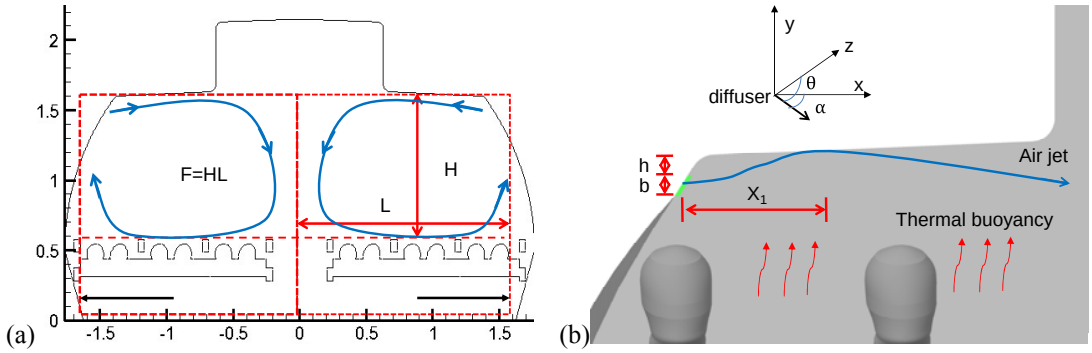

Fig. 5. Three-dimensional characteristic of the wall jet in a cabin.

In reality, the wall jet in cabins cannot be of two-dimensional flow because of the complicated geometry and three-dimensional supply air from the diffusers. The geometry characteristic factor of the wall-attachment air jet under a non-isothermal condition is defined as:

$$Z = 9.6\sqrt[3]{b\frac{(mu)^4}{(n\Delta T)^2}} \tag{3}$$

The wall attachment length can be expressed as:

$$X_1 = 0.5ZEXP(K) \tag{4}$$

where $K = 0.7 - 0.35h/b$, $m = 2.5*\sqrt{2}$, and $n = 2*\sqrt{2}$.

Based on the experiment results, the wall attachment length considers the 3D characteristic of the air supply:

$$X_1 = 0.5ZEXP(K)(\cos^2\theta\cos\alpha) \tag{5}$$

Based on the analysis above, corrected Ar_{sc} and Re are proposed to evaluate the airflow in the cabins:

$$Ar_{sc} = \frac{\beta gF(T_i - T_f)}{(u_d\cos^2\theta\cos\alpha)^2} \tag{6}$$

$$\mathrm{Re}_d(effective) = \frac{u_d h}{\nu}\cos^2\theta\cos\alpha \tag{7}$$

3. Results

3.1 Ventilation performance

As shown in Table 1, the ventilation rate in the cabin mockup was 45.8 h^{-1}, and it was closer to the real cabin condition of 43.7 h^{-1} in the MD-82. It should be noted that the supply air volume in different environmental cabins is difficult to keep consistent. Cao et al. [8] concluded that the jet behaviors in a cabin mockup can be compared under a series of supply air volumes. The mass and heat transfer equilibrium in the two cabins were calculated, as shown in Table 1. Both the mass balance and thermal equilibrium ratios for the two cabins were less than 10%, indicating an acceptable heat and mass balance for maintaining a stable

thermal environment. Moreover, it can be concluded that the seven-row cabin mockup had a better mass balance and heat transfer equilibrium.

Table 1 Mass and heat transfer balance in the two cabins.

	Cabin mockup	MD-82
Supplied ventilation volume [m³/h]	1529	4888
Exhaust ventilation volume [m³/h]	1442	4544
Ventilation rate [/h]	45.8	43.7
Mass balance ratio	5.7 %	7.0 %
Heat equilibrium ratio	7.0 %	9.5 %

The measured air velocity magnitude and longitudinal velocity distribution in the upper areas of the cross sections (above the floor within 0.6-1.35 m) of the two cabins are shown, respectively, in Figs. 6(a) and 6(b). The experimental data of each cabin included three rows and were measured with UAs. The Standard 161–2007(ASHRAE) [37] demands that the local air speed of the seated passengers and crew be below than 0.36 m/s. Besides, the minimum bare body areas encountered an air speed of 0.1 m/s, and a maximum speed of 0.3 m/s is recommended. Figure 6(a) shows that over 90% of the measuring points situated in the seated passenger and crew areas have velocities below than 0.36 m/s in the two cabins. In addition, the air velocity with the recommended magnitude (0.1-0.3 m/s) accounted for 60% in the cabin mockup. However, the recommended magnitude only accounted for 30% in the MD-82. This result indicates that both cabins meet the requirement of the Standard 161–2007(ASHRAE) [37], but this cabin mockup is more suitable for investigating the ventilation perform. Fig. 6(b) shows that most points in the two cabins have a longitudinal velocity between -0.15 and 0.15 m/s, and the longitudinal velocity distribution ratio is similar. This phenomenon provides evidence that the 7-row cabin mockup is sufficient to reflect longitudinal flow in real cabins.

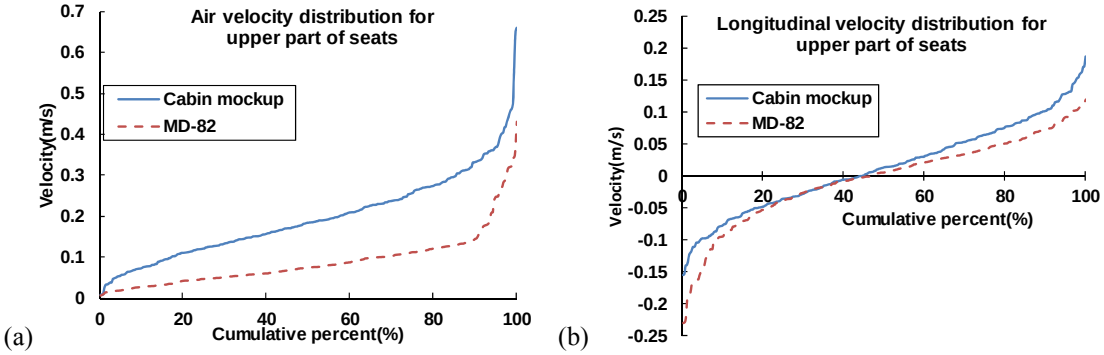

Fig. 6. Measured velocity characteristics in the upper areas of the cross section of the two cabins (above the floor within 0.6-1.35 m): (a) air velocity magnitude and (b) longitudinal velocity.

3.2 Comparison of velocity field by UAs and PIV

In the cabin mockup, the airflow field was measured twice by UAs and 2D-PIV under

the cooling condition. The velocity vectors were equal to $\sqrt{U_x^2 + V_y^2}$. PIV focuses on the 2D flow field, where U_x and V_y are the two mean velocity components in the cross section. In reality, large-scale PIV cannot be used in real cabins, such as the MD-82, because of the non-transparent materials. Therefore, it is essential to compare the measured velocity field by the UAs and PIV to guarantee the reliability of the comparison between the two cabins. Fig. 7 shows the comparison of the measured velocity field by the PIV and the UAs at the section of Row 4. Fig. 7(a) compares the velocity vectors, exhibited similar characteristics and airflow pattern. Seven lines were chosen to compare the magnitude of the velocity by the two measuring tools. As depicted in Fig. 7(c), the velocity vectors had larger differences in the aisle (Line 1 through 3). Li et al. [11] applied PIV to measure the jet collision region (Fig. 3(c)) in a central aisle. They found unsteady flow features, such as unstable periodic swing motion and the interaction of the two lateral jets in the aisle. The UAs measurement system just get three points velocity once, so it hard to get the full velocity field in the aisle, especially the jet collision region. There is also why the measured velocity magnitude by the UAs in the Line 1 suddenly smaller, on the contrary, the measured velocity magnitude by the UAs in the Line 2 suddenly grew larger. So the disagreement between different experimental methods in Line 1 and Line 2 is great. And the disagreement is also obvious in some parts of Line 3, but other parts shows a good agreement. Fig. 7(d) and Fig. 7(e) presents the two measured velocity profiles were parallel in the occupied zone. But the velocity measured with the UAs near the core region of the wall jet was much lower, because of the jet decay from the diffusers to the UA probe. Therefore, UA measurements may lead to inaccurate velocity results in the unsteady flow region as a result of local perturbations by the large UA probes. Moreover, it was found that the high-resolution PIV data were more useful for quantifying the air jet behaviors in the present study.

To quantify the differences, the normalized root-mean-square deviations (NRMSDs) [38] were calculated using Eq. (8),

$$NRMSD = \frac{\sqrt{(\sum_{i=1}^{n}(C_{PIV,i} - C_{UA,i})^2) / n}}{C_{PIV,\max} - C_{PIV,\min}} \tag{8}$$

The value was approximately 11.54%, indicating that the velocity profiles measured by PIV and the UAs were quite similar. As shown in Fig. 7(a), most of the discrepancy came from the data in the aisle. Nevertheless, the UAs provide results with reasonable accuracy in the cross section as a whole, and these results can be a useful supplement to the PIV measurements.

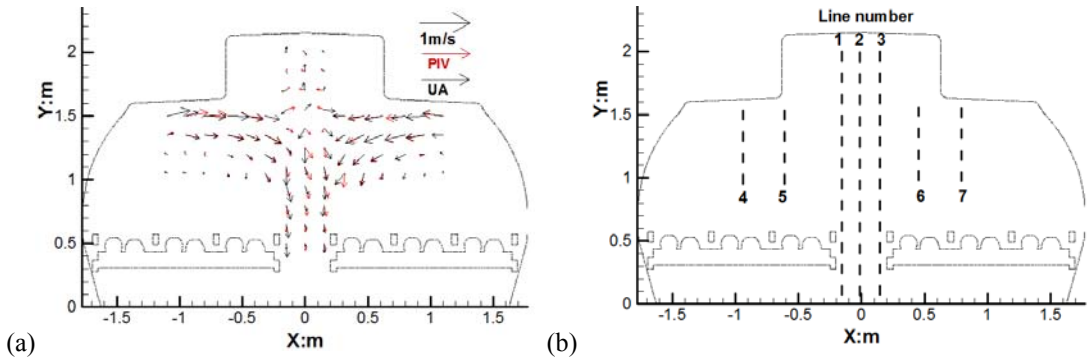

(a) (b)

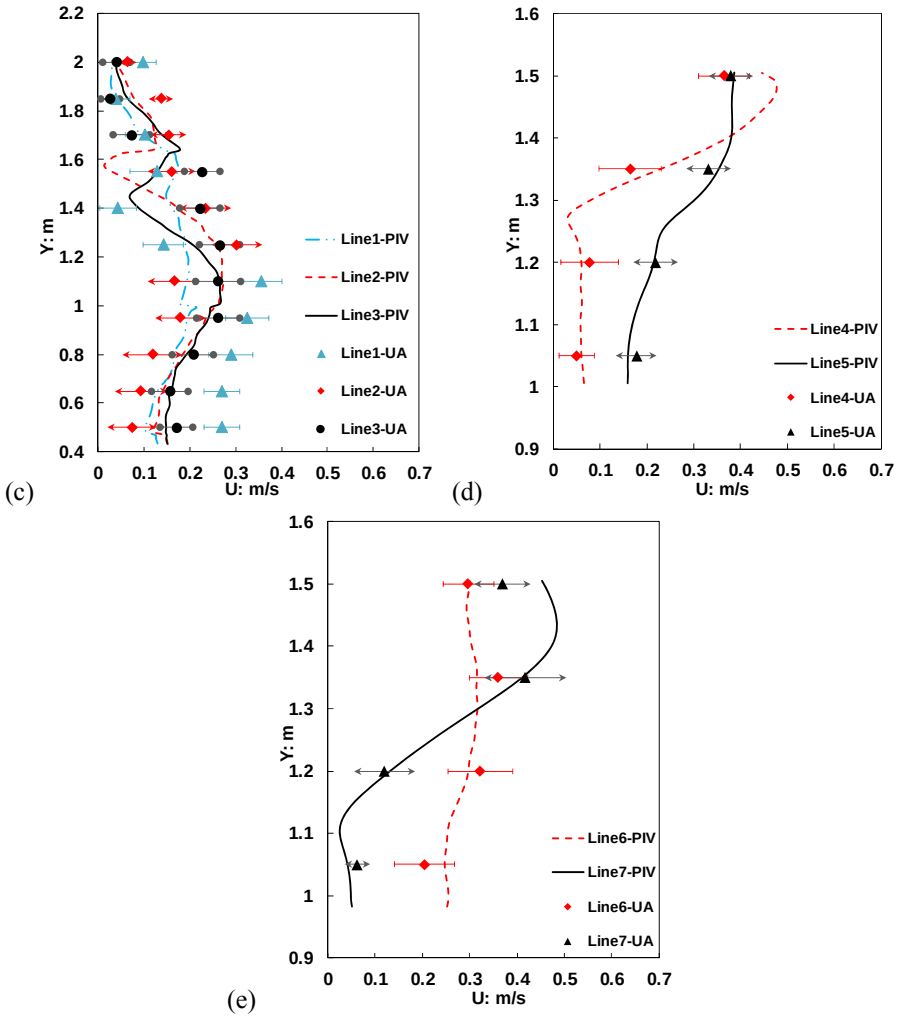

Fig. 7. Comparison of air velocity magnitude by the UAs and PIV in Row 4.

In the MD-82, the sampling grid resolution was 0.1 m × 0.1 m for the measured planes, higher than in the cabin mockup. Hence, the reliability of the experimental data with UAs and PIV in the two cabins was guaranteed and verified.

3.3 Airflow field of the diffusers

To examine the similarity of the linear slot diffusers between the two cabin facilities, we conducted PIV measurements of the airflows from the two sets of diffusers under isothermal conditions in part 5 of section Row 4, which was a typical section. The schematic model of the original and modified diffusers in the cabin mockup is shown in Fig. 2. Fig. 8 (a) and Fig. 8 (b) compare the measured velocity vectors and TI in part 5, respectively. To quantify the differences, the NRMSD of the velocity magnitude and TI were calculated using Eq. (9), and the values were approximately 7.24% and 9.12%, respectively.

$$NRMSD = \frac{\sqrt{\left(\sum_{i=1}^{n}\left(C_{Original,i} - C_{Modified,i}\right)^2\right) / n}}{C_{Original,\max} - C_{Modified,\min}} \tag{9}$$

The comparison of measured velocity vectors and TI shows that the two diffuser types were almost identical, and indicates that the diffuser difference has little effect on the airflow field. Comparing the schematic model of the modified diffuser in the cabin mockup and the diffuser in the MD-82, the height of linear slot is 22 mm for both and arranged in two rows. Hence, the gaps between the diffusers in the upper and lower rows in the MD-82 can be ignored in this study, so we defined the characteristic dimension of the diffuser in the MD-82 as 50 mm.

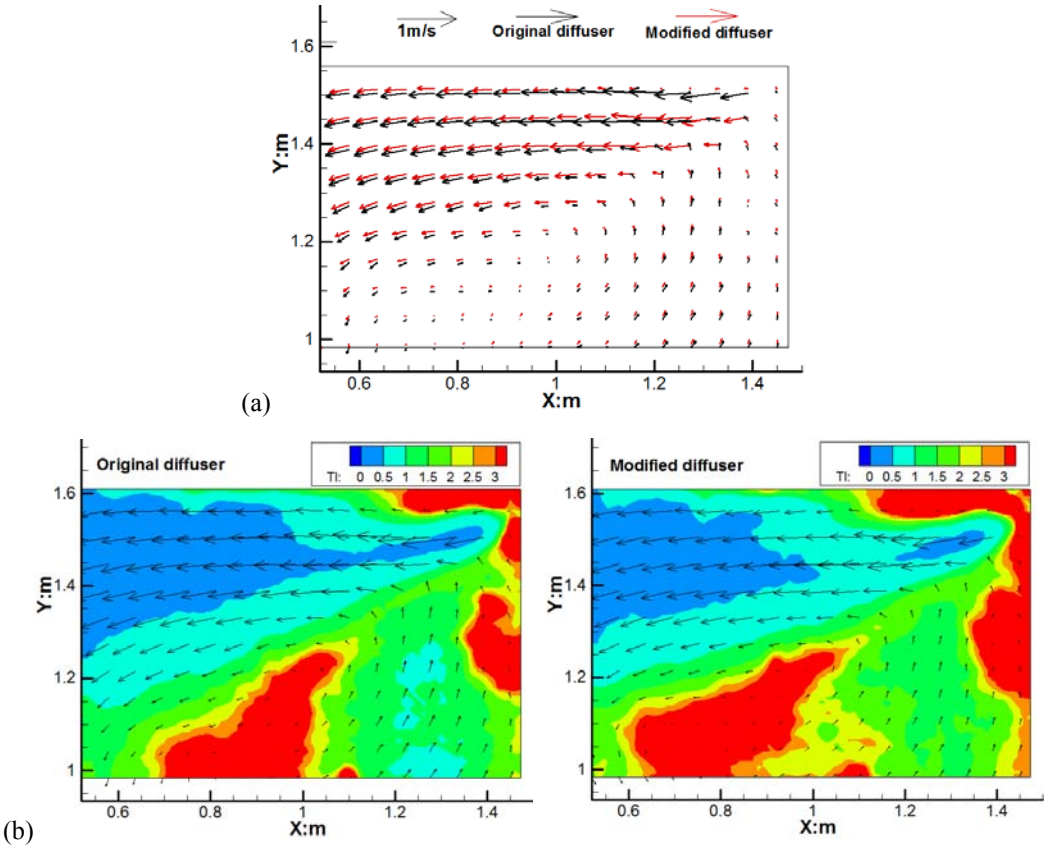

Fig. 8. (a) Comparison of the measured air velocity vectors of part 5 in section Row 4 and (b) comparisons of the measured turbulence intensity (TI) of part 5 in section Row 4.

3.4 Airflow pattern

In a previous study [11], there was no significant difference in the airflow pattern of the cross sections in the cabin mockup. Therefore, the PIV measurements were only conducted on the cross section of Row 4 at different supply air volumes, varying from 2.3 to 9.4 L/(per·s). Fig. 9 shows the flow fields at six supply air volumes. As the air supply volume decreased, two jet flow from the diffusers did not merge at the aisle, such as 2.3 to 5.3 L/(per·s), so only the A-side air jet was measured, which included part 3 and part 5. Fig. 10 depicts the measured velocity field in the three cross planes of the MD-82, showing that only CS5 achieved the original design intention and the asymmetric distribution of the seats in both sides generated the asymmetric airflow in both sides. This pattern was significantly

different from the measurement results in the first-class cabin [5]. The airflow patterns in the other sections were similar to the flow structure at air supply air rates varying from 2.3 to 5.3 L/(per·s) in the cabin mockup. Therefore, the results compared the airflow pattern in the two cabins.

	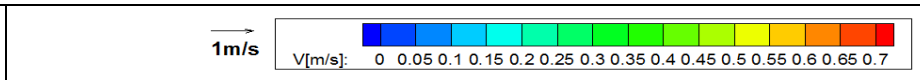					
Re_d(e)	5750	5126	4250	3876	3813	3500
Ar_{sc}	0.050	0.063	0.123	0.133	0.152	0.163
U_d/(m/s)	1.81	1.61	1.53	1.36	1.41	1.25
	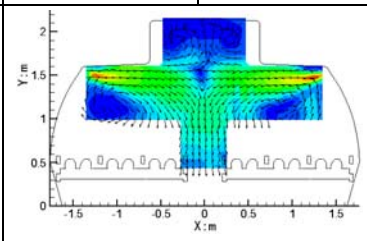		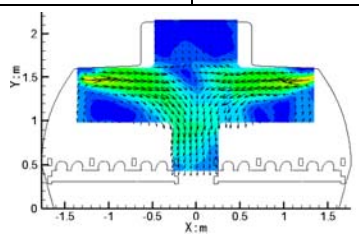		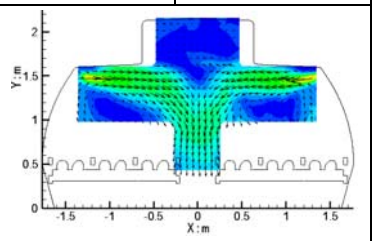	
	a-R4(9.4 L/(per•s))		b-R4(7.9 L/(per•s))		c-R4(7.1 L/(per•s))	
Re_d(e)		2781		1906		1406
Ar_{sc}		0.286		0.609		1.119
U_d/(m/s)		0.88		0.57		0.45
	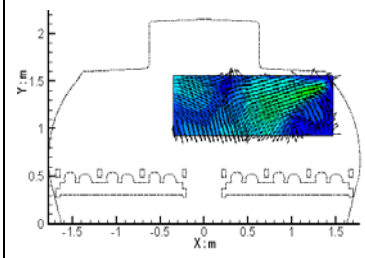		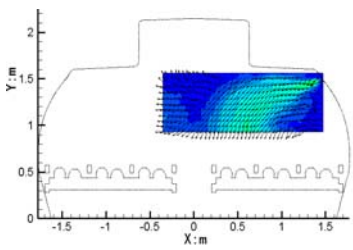		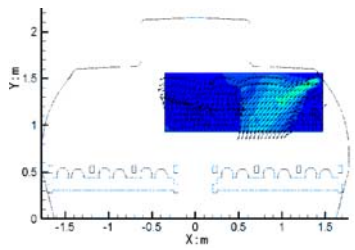	
	d-R4(5.3 L/(per•s))		e-R4(3.3 L/(per•s))		f-R4(2.3 L/(per•s))	

Fig. 9. Measured flow field in the cross sections: Cabin mockup.

	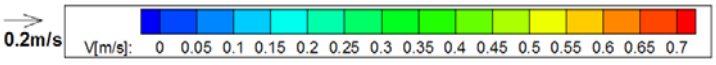					
Re_d(e)	1420	2221	960	857	3438	2352
Ar_{sc}	1.194	0.370	2.614	2.479	0.154	0.33
U_d/(m/s)	0.99	1.45	0.85	0.51	1.47	1.36
	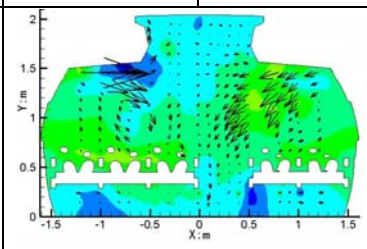		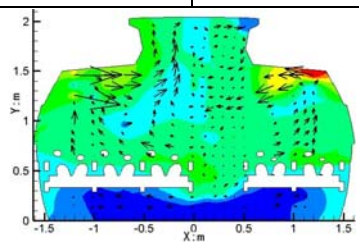		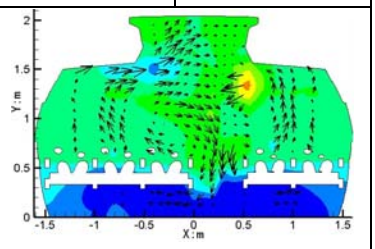	
	CS3		CS4		CS5	

Fig. 10. Measured flow field in the cross sections: MD-82.

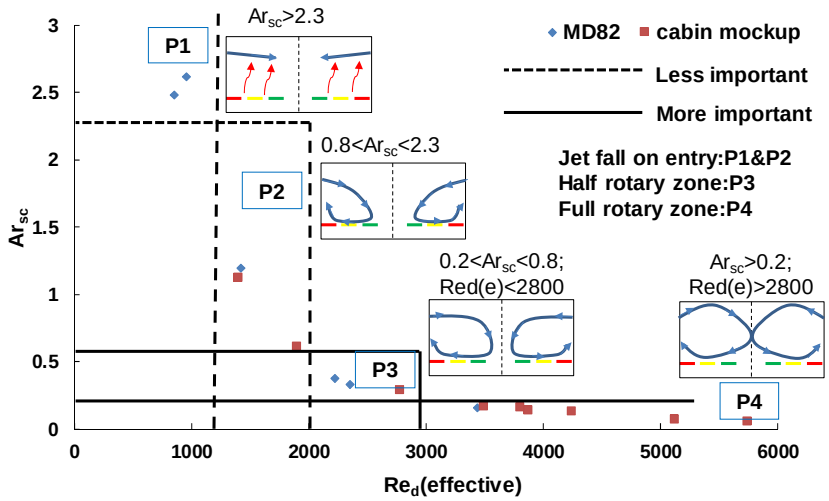

Fig. 11. Summary of the condition to maintain a certain type of airflow pattern.

In this study, Ar_{sc} and Re_d(effective) were introduced to describe the airflow pattern. The values were calculated by Eqs. (6) and (7), and they are shown in Fig. 9 and Fig. 10. Then, the condition (thermal buoyancy and inertia force) was obtained to maintain a certain type of airflow pattern, as shown in Fig. 11. There were four stage airflow patterns in the cabins. The full rotary zone, corresponding to the fourth airflow pattern (P4), existed at critical $Ar_{sc} < 0.2$ and Re_d(effective) > 2800. At this zone, the air jets from the diffusers merged at the aisle, which achieved the original design intention. At critical Re_d(effective) < 2800, as the inertia force decreased, the buoyancy forces destroyed the air draft pattern. As a result, the air-jet fell on full entry. In the cabin mockup, under the cruise condition (9.4 L/(per·s)), the airflow was the original design intention. However, as the air supply volume decreased, there were three types of airflow patterns, P2, P3 and P4. To maintain full rotary flow in the MD-82, the critical Re_d(effective) should be larger than 2800, and the air supply average velocity should be below 1.07 m/s. Although the average air speed from the diffusers was 1.12 m/s, the air supply along the longitudinal direction was different. Therefore, most sections were falls on entry, such as the left side of CS4. The U_d(effective) was 0.3 m/s, corresponding to an supply air volume of 2.0 L/(per·s). Under the asymmetrical air supply boundary, there existed three types of airflow patterns, P1, P2 and P3. The result depicted in Fig. 11 illustrates that the experiment in the cabin mockup can reflect the flow characteristics of mixing ventilation in a real aircraft cabin. The results also indicate that the inertia force of the air jet from the diffuser Re_d(effective) is the dominant variable for the airflow pattern.

4. Discussion

This investigation also analyzed the simulation system confidence, and there are three similarity theorems. The first similarity theorem tells us that the similitude criterions should be equal for two similar phenomena. The third similarity theorem tells us that, other than the equal similitude criterions, their single valued condition, such as the geometry, should also be the same. The second similarity theorem tells us that the similitude criterions containing

physical quantities have a function relationship. In this study, the experimental condition was controlled to be the same as a real aircraft cabin by ECS in the cabin mockup. Therefore, these mockup cabins satisfied the requirement of mechanical similarity. However, for the simulation system confidence, ventilation similarity was not only needed to meet the requirement of mechanical similarity but also to represent the general airflow features of the aircraft cabin and reflect the phenomena and characteristics resulting from these features.

In this study, the cabin mockup and MD-82 were not the same aircraft model. The cabin mockup was based on the Boeing 737, it is one of the most popular aircraft model in the world. Although the MD-80 series of aircraft only represent a small portion of the current fleet of commercially operated passenger planes [39], the ventilation form is still the mainstream in real cabins, same as the Boeing 737. Obviously, it was quite difficult to achieve strict geometric similarity, and some aspects were neglected, such as the influence of the seat arrangement and manikins on the airflow. This study focused on the most important parameters and flow field characteristics. Although the comparison of the airflow field measured by PIV for each diffuser type showed that the gaps between the diffusers in the upper and lower rows can be ignored, the gaps between the diffusers in adjacent rows are not discussed here. Li et al. [11] found that the gaps between the diffusers were the direct cause of the aisle airflow patterns. In addition, similar to many other studies [10, 23, 40], this study only listed the airflow pattern measured in the cross planes of an MD-82 and a cabin mockup. Liu et al. [5] and Zhang et al. [14, 21] used UAs to measure the air velocity field in the first-class cabin of this MD-82 and a cabin mockup, respectively. Although the two cabins only contained three rows of seats, there was obvious longitudinal flow. The longitudinal flow can enhance the air pollutant dispersion in an aircraft cabin. Hence, a comparison of the longitudinal airflow field and transition regulation characteristic of the contaminant between the cabin mockup and real aircraft cabin will be the focus of future investigations.

5. Conclusions

This investigation described a method procedure and similitude criteria to compare the ventilation in a cabin mockup and a real cabin. Our work drawn the following conclusions.

a) In the cabin mockup, the air distributions of the cross sections by PIV and UA both exhibited similar characteristics and reflected the airflow pattern. In general, PIV performs better than UAs in measuring the airflow field of cabins because of the high resolution and non-contact measurement. Nevertheless, UAs provide results with reasonable accuracy in the cross section as a whole, and this data can be a useful supplement to PIV measurements.

b) By comparing the velocity vectors and TI measured between the original and modified diffuser in the cabin mockup, it was found that the simplified diffuser did not have a significant effect on the airflow under the same air supply volume in the cabin. Hence, the gaps between the diffusers in the upper and lower rows in the MD-82 could be ignored in this study by defining h_{slot} as the characteristic dimension of the diffuser in the two cabins.

c) With the single aisle layouts and mixing ventilation system, similar phenomena and similitude criteria verified that this cabin mockup can be accurate enough to represent a real cabin environment and could be better used in the study of ventilation. Under similar ventilation rates, the air with the recommended magnitude (0.1-0.3 m/s) accounted for 60% in

the mockup cabin, which is 30% larger than that in the MD-82. Most points in the two cabins have a longitudinal velocity between -0.15 and 0.15 m/s, and the longitudinal velocity distribution ratio was similar. With different air supply boundary conditions, there were four types of airflow patterns in the cabin mockup and MD-82. And the airflow pattern in the cabins could be described with the modified Reynolds number (Ar_{sc}) and Archimedes number (Re_d (effective)).

Acknowledgment

This study was supported by the Tianjin Key Fundamental Research Program through grant no. 14JCZDJC39200 and the National Basic Research Program of China (The 973 Program) through Grant No. 2012CB720100. The authors would like to thank Dr. Chao-Hsin Lin and Dr. Daniel Wei from the Boeing Company for the technical support and funding in the experiment.

References

[1] UNWTO, UNWTO World Tourism Barometer, 2013.

[2] W. Cui, Q. Ouyang, Y. Zhu, Field study of thermal environment spatial distribution and passenger local thermal comfort in aircraft cabin, Build. Environ. 80 (2014) 213-220.

[3] F. Li, J. Liu, J. Pei, C.-H. Lin, Q. Chen, Experimental study of gaseous and particulate contaminants distribution in an aircraft cabin, Atmos. Environ. 85 (2014) 223-233.

[4] F. Li, B. Li, J. Liu, Measuring and containing longitudinal flow: Important for airborne pollutants control in an aircraft cabin, Science and Technology for the Build. Environ. 21 (2015) 1126-1133.

[5] W. Liu, J. Wen, J. Chao, W. Yin, C. Shen, D. Lai, C.-H. Lin, J. Liu, H. Sun, Q. Chen, Accurate and high-resolution boundary conditions and flow fields in the first-class cabin of an MD-82 commercial airliner, Atmos. Environ. 56 (2012) 33-44.

[6] C. Shen, J. Liu, W. Wang, N. Jiang, Experimental Measurement of Airflow Turbulence Characteristics in a Full-Size Aircraft Cabin, In: Proceedings of the 8th international symposium on heating, ventilation and air conditioning. Springer, (2014) 341-349.

[7] B. Li, R. Duan, J. Li, Y. Huang, H. Yin, C. H. Lin, D. Wei, X. Shen, J. Liu, Q. Chen, Experimental studies of thermal environment and contaminant transport in a commercial aircraft cabin with gaspers on, Indoor air. (2015).

[8] X. Cao, J. Liu, J. Pei, Y. Zhang, J. Li, X. Zhu, 2D-PIV measurement of aircraft cabin air distribution with a high spatial resolution, Build. Environ. 82 (2014) 9-19.

[9] X. Cao, J. Li, J. Liu, W. Yang, 2D-PIV measurement of isothermal air jets from a multi-slot diffuser in aircraft cabin environment, Build. Environ. 99 (2016) 44-58.

[10] M. Kühn, J. Bosbach, C. Wagner, Experimental parametric study of forced and mixed convection in a passenger aircraft cabin mock-up, Build. Environ. 44 (2009) 961-970.

[11] J. Li, X. Cao, J. Liu, C. Wang, Y. Zhang, Global airflow field distribution in a cabin mock-up measured via large-scale 2D-PIV, Build. Environ. 93 (2015) 234-244.

[12] C. Lin, T. Wu, R. Horstman, P. Lebbin, M. Hosni, B. Jones, B. Beck, Comparison of large eddy simulation predictions with particle image velocimetry data for the airflow in a generic cabin model, HVAC&R Res. 12 (2006) 935-951.

[13] L. Pang, J. Xu, L. Fang, M. Gong, H. Zhang, Y. Zhang, Evaluation of an improved air distribution system for aircraft cabin, Build. Environ. 59 (2013) 145-152.
[14] T. Zhang, P. Li, S. Wang, A personal air distribution system with air terminals embedded in chair armrests on commercial airplanes, Build. Environ. 47 (2012) 89-99.
[15] J. Fišer, M. Jícha, Impact of air distribution system on quality of ventilation in small aircraft cabin, Build. Environ. 69 (2013) 171-182.
[16] J. Bosbach, J. Pennecot, C. Wagner, M. Raffel, T. Lerche, S. Repp, Experimental and numerical simulations of turbulent ventilation in aircraft cabins, Energy. 31 (2006) 694-705.
[17] A. Baker, S. Ericson, J. Orzechowski, K. Wong, R. Garner, Aircraft passenger cabin ECS-generated ventilation velocity and mass transport CFD simulation: velocity field validation, Journal of the IEST. 49 (2006) 51-83.
[18] H. Mo, M. Hosni, B. Jones, Application of particle image velocimetry for the measurement of the airflow characteristics in an aircraft cabin, ASHRAE Trans. 109 (2003) 101-110.
[19] W. Liu, S. Mazumdar, Z. Zhang, S. B. Poussou, J. Liu, C.-H. Lin, Q. Chen, State-of-the-art methods for studying air distributions in commercial airliner cabins, Build. Environ. 47 (2012) 5-12.
[20] C.-H.-. Lin, K. Dunn, R. Horstman, J. Topmiller, M. Ahlers, J. Bennett, L. Sedgwick, S. Wirogo, Numerical Simulation of Airflow and Airborne Pathogen Transport in Aircraft Cabins--Part I: Numerical Simulation of the Flow Field, ASHRAE Trans. 111 (2005).
[21] Z. Zhang, X. Chen, S. Mazumdar, T. Zhang, Q. Chen, Experimental and numerical investigation of airflow and contaminant transport in an airliner cabin mockup, Build. Environ. 44 (2009) 85-94.
[22] R. P. Garner, K. L. Wong, S. C. Ericson, A. Baker, J. A. Orzechowski. CFD validation for contaminant transport in aircraft cabin ventilation flow fields, In: Proceedings of Annual SAFE Symposium on Survival and Flight Equipment Association, (2004) 248-253.
[23] J. Bosbach, S. Lange, T. Dehne, G. Lauenroth, F. Hesselbach, M. Allzeit, Alternative ventilation concepts for aircraft cabins, CEAS Aeronautical Journal. 4 (2013) 301-313.
[24] C. Butler, D. Newport, Experimental and numerical analysis of thermally dissipating equipment in an aircraft confined compartment, Appl. Therm. Eng. 73 (2014) 869-878.
[25] P. Zítek, T. Vyhlídal, G. Simeunović, L. Nováková, J. Čížek, Novel personalized and humidified air supply for airliner passengers, Build. Environ. 45 (2010) 2345-2353.
[26] A. Wang, Y. Zhang, Y. Sun, X. Wang, Experimental study of ventilation effectiveness and air velocity distribution in an aircraft cabin mockup, Build. Environ. 43 (2008) 337-343.
[27] L. Zhao, Y. Zhang, X. Wang, G. L. Riskowski, Analysis of Airflow in a Full-Scale Room with Non-Isothermal Jet Ventilation Using PTV Techniques, ASHRAE Trans. 113 (2007).
[28] L. Albright, Air flow through hinged baffle slotted inlets, Trans. ASAE. 19 (1976) 728-0732.
[29] Y. Jin, J. Ogilvie, Airflow characteristics in the floor region of a slot ventilated room (isothermal), Trans. ASAE. 35 (1992) 695-702.
[30] D. Pattie, W. Milne, Ventilation air-flow patterns by use of models, Trans. ASAE. 9 (1966) 646-0649.
[31] M. Timmons, G. Baughman, Similitude analysis of ventilation by the stack effect from an open ridge livestock structure, Trans. ASAE. 24 (1981) 1030-10340.
[32] W. Yao, L. Christianson, A. Muehling, Air movement in neutral pressure swine buildings: similitude theory and test results, American Society of Agricultural Engineers Microfiche collection (USA). (1986).
[33] H. Yu, L.-J. Jou, H.-T. Ouyang, H.-M. Liang, C.-M. Liao, Similitude Criteria for a Two-dimensional Wall Jet in an Isothermal Mechanically Ventilated Enclosure, Biosyst. Eng. 93 (2006) 415-425.
[34] J. Wang, J. Ogilvie, Design guidelines for airflow patterns in slot-inlet rooms: non-isothermal. ASAE Paper,

94 (1994) 4534.
[35] H. Yu, Trajectory of a Horizontally Diffused Plane Wall Jet in a Non-isothermal Ceiling Slot-ventilated Enclosure, Biosyst. Eng. 91 (2005) 99-109.
[36] B. Tripathi, S. Moulic, Investigation of air drafting pattern obtained from the variation in outlet positions inside a closed area, J. Appl. Fluid Mech. 5 (2012) 1-12.
[37] ASHRAE, Standard 161–2007, Air Quality within Commercial Aircraft, ASHRAE, Inc, Atlanta, 2007.
[38] http://cirpwiki.info/wiki/Statistics.
[39] http://www.airportspotting.com/airlines-fly-md80-series/.
[40] W. Yan, Y. Zhang, Y. Sun, D. Li, Experimental and CFD study of unsteady airborne pollutant transport within an aircraft cabin mock-up, Build. Environ. 44 (2009) 34-43.